Carrier relaxation and recombination in an InGaN/GaN quantum well probed with time-resolved cathodoluminescence

X. Zhang, D. H. Rich,[a] J. T. Kobayashi, N. P. Kobayashi, and P. D. Dapkus[b]
Department of Materials Science and Engineering, University of Southern California, Los Angeles, California 90089-0241

(Received 8 June 1998; accepted for publication 10 July 1998)

Spatially, spectrally, and temporally resolved cathodoluminescence (CL) techniques have been employed to examine the optical properties and kinetics of carrier relaxation for metalorganic chemical vapor deposition grown InGaN/GaN single quantum wells (QWs). Cathodoluminescence wavelength imaging of the QW sample revealed local band gap variations, indicating the presence of local In composition fluctuations and segregation during growth. A detailed time-resolved CL study shows that carriers generated in the boundary regions will diffuse toward and recombine at InN-rich centers, resulting in a strong lateral excitonic localization prior to radiative recombination.
© *1998 American Institute of Physics.* [S0003-6951(98)03936-9]

The study of InGaN/GaN heterostructures and quantum wells (QWs) has in recent years drawn a great deal of interest, owing to the rapid progress and realization of high quality blue and green InGaN single QW light emitting diodes[1] and room-temperature pulse operation of InGaN single[2] and multiple[3] QW laser diodes. Time-resolved photoluminescence has been used to study the radiative recombination in InGaN single[4,5] and multiple[6] QW structures. Several authors observed that the emission results mainly from recombination of excitons localized at certain potential minima originating from large $In_xGa_{1-x}N$ compositional fluctuations caused by phase separation.[6–8] Direct evidence for exciton localization was shown in InGaN single QWs by Chichibu *et al.*[9] However, the effects of the InGaN composition undulation on the carrier diffusion, relaxation, and recombination of localized excitons are far from being well understood, particularly in the boundary regions between centers of exciton localization.

In this study, we have employed spatially, spectrally, and temporally resolved cathodoluminescence (CL) to investigate the carrier relaxation and recombination in an InGaN/GaN single QW sample. Cathodoluminescence wavelength imaging (CLWI)[10] measurements were performed to assess the spatial extent of the band gap variations caused by the In composition fluctuations. We will show that for low excitation conditions, CLWI revealed local In composition fluctuations on a scale of less than ~100 nm, which is indicative of a strong carrier localization at InN-rich centers. The impact of the large $In_xGa_{1-x}N$ compositional fluctuations on the spatial variation of the luminescence intensity and lifetimes as well as carrier transport and capture process is explored.

The 4-nm-thick InGaN single QW sample was grown by atmospheric pressure metalorganic chemical vapor deposition using a closed space showerhead reactor via multistep growth approach[11] on a sapphire (0001) substrate, followed by a 70-nm-thick GaN capping layer. The undoped QW sample has a 15% average In composition.

The CL experiments were performed with a modified JEOL-840A scanning electron microscope using a 10 keV electron beam with various probe currents.[12] CLWI was performed by acquiring a series of discrete monochromatic images, constructing a local spectrum at all 640×480 scan points within the image, and determining the wavelength, $\lambda_m(x,y)$, at which there is a peak in the CL spectrum at each scan point *(x,y)*. CLWI thus enables a spatial mapping of the effective band gap, which can vary as a result of strain and alloy fluctuations.[10] The temperature of the sample was maintained at 93 K. Our CL system with time-resolved capability has been described previously,[12] and time-resolved CL experiments were performed with the method of delayed coincidence in an inverted single photon counting mode with a time resolution of ~100 ps. Electron beam pulses of 50 ns width with a 1 MHz repetition rate were used to excite the sample. The luminescence signal was dispersed by a 0.25-m monochromator and detected by a cooled GaAs:Cs PMT.

Spatially averaged CL spectra, acquired under various

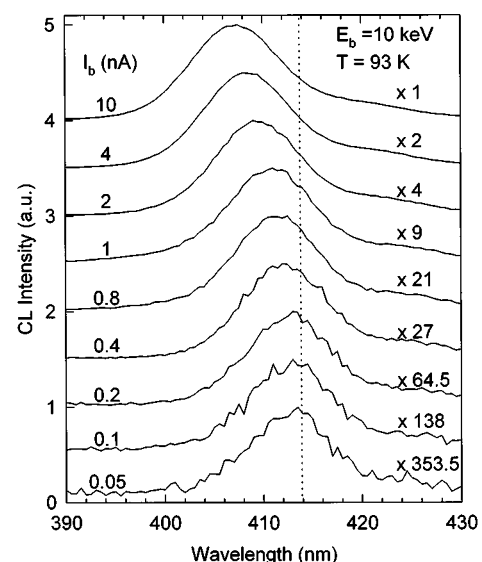

FIG. 1. Stack plots of normalized CL spectra taken with various probe currents.

[a]Author to whom correspondence should be addressed.
[b]Also with Department of Electrical Engineering/Electrophysics.

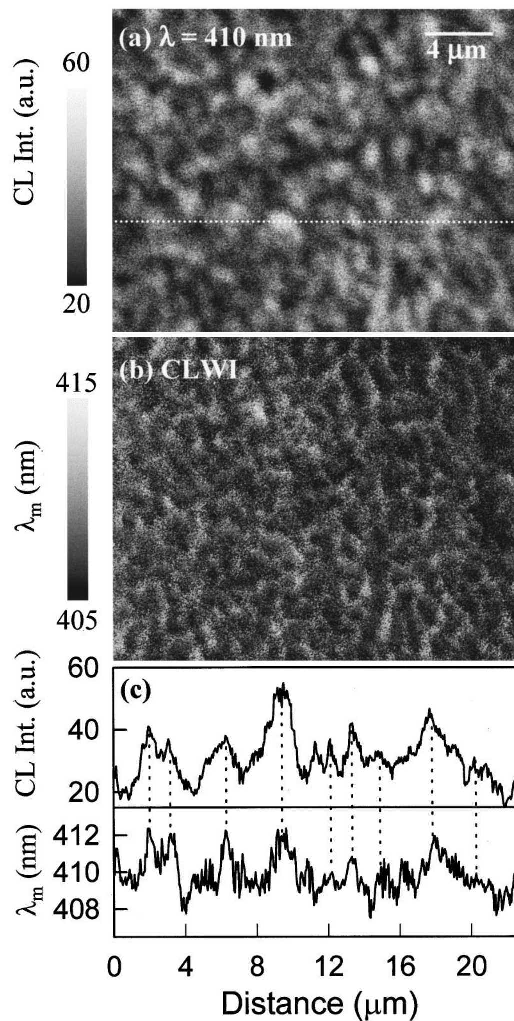

FIG. 2. (a) Monochromatic CL image, (b) CLWI image, and (c) line scan analysis for an e-beam current of 1 nA. The gray-scale bar serves as a key for the wavelength mapping in (b). The CL intensity of the scan at 410 nm and the peak wavelength, λ_m, along the dashed line in (a) are shown in (c).

excitation currents (I_b) are shown in Fig. 1. The beam currents vary from 0.05 to 10 nA and the beam was raster scanned over an area of $25.6\times18.8\ \mu\text{m}^2$. All spectra are normalized to have the same intensity; the scaling factors are indicated to the right of each spectrum. The peak position of the QW emission shifts toward shorter wavelengths as the beam current increases, resulting in a ~51.4 meV blueshift as the beam current is increased from 0.05 to 10 nA. This effect can be attributed to the rapid band filling of localized $In_xGa_{1-x}N$ radiative centers composed of large In concentrations. The full widths at half maximum of these spectra also increase from 80.0 to 87.5 meV in the 0.05–10 nA range.

Scanning monochromatic CL and CLWI images for a scanned area of $25.6\times18.8\ \mu\text{m}^2$ are shown in Fig. 2. The spotty nature of the monochromatic CL images, showing distinct bright and dark emission regions, is consistent with a strong localization of excitons prior to radiative recombination.[9] Figure 2(b) shows corresponding CLWI image of the same region of Fig. 2(a). The mapping of λ_m into a color-scale representation is shown by the gray-scale bar indicating the wavelength scale. A spatial correlation between the bright regions of the monochromatic CL images and longer wavelength regions of CLWI is observed, as

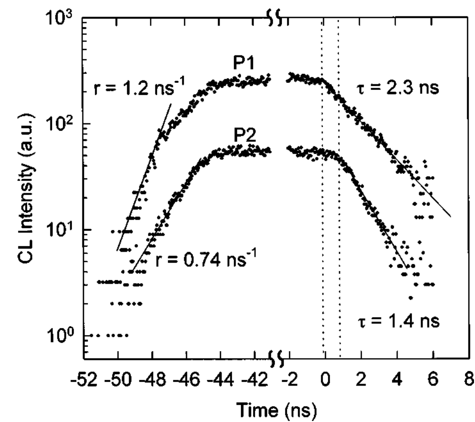

FIG. 3. CL transients including the onset and decay of the 410 nm luminescence taken near an exciton localization center (P1) and dark boundary region (P2).

shown in the line scan analysis of Fig. 2(c). The correlation, as illustrated by the dashed vertical lines, shows that carrier localization in the InGaN QW is due to the spatial variation of the In composition and an attendant band gap variation.

Cathodoluminescence imaging further revealed that the sizes of the bright and dark regions depend on the level of excitation. That is, the minimum feature size scales by a factor of ~2 as the beam current is increased from 0.3 to 1 nA. The increase in the feature size is evidently related to the rapid band filling of carriers in InN-rich regions, which should change the spatial shape of the potential variation in the vicinity of the InN-rich centers and alter the subsequent drift and diffusion of carriers towards the lowest energy minima.

In order to further understand the spatial variation in the carrier relaxation and recombination, time-resolved CL was performed by positioning the electron beam in varying proximity to the bright luminescence centers and dark boundary regions observed in Fig. 2(a). Transients of the CL intensity decay versus time were acquired at various positions relative to exciton localization centers. Figure 3 shows typical transients, denoted as P1 and P2, corresponding to the e beam positioned to a bright center and dark boundary regions, respectively. The CL decay lifetimes are obtained by fitting the initial decay with a constant lifetime, as shown in the semilogarithmic plots of Fig. 3. The fits indicate that the region corresponding to P1 exhibits a longer lifetime (2.3 ns) than the region corresponding to P2 (1.4 ns). A spatial dependence of the lifetime was examined by acquiring a set of transients along an arbitrary line in an e-beam line scan. Figure 4(a) shows again a line scan analysis of the CL intensity at λ=410 nm for a scan of ~25 μm in length. The dots in Fig. 4(b) show the corresponding decay times of the 412 nm emission at various e-beam positions along the same line. The positions of the transients denoted as P1 and P2 in Fig. 3 are also indicated in Fig. 4(a).

A strong correlation is observed between the CL intensity and carrier lifetime in Fig. 4. The carrier lifetimes are generally longer and shorter for higher and lower CL intensities, respectively, along the line scan. The reduced lifetime in the darker boundary regions can be attributed to defects or impurities acting as nonradiative centers which reduce the total lifetime of excess carriers.

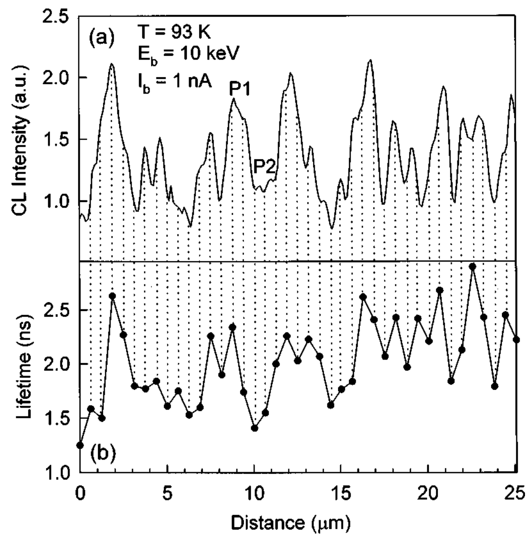

FIG. 4. (a) CL intensity of the 410 nm luminescence and (b) lifetimes vs distance for an e-beam line scan.

A closer examination of the CL transients P1 (bright region) and P2 (dark region) in Fig. 3 shows marked differences during the onset and the initial stages of the intensity decay. We define an onset rate, r, as $r=\Delta\ \ln(I_{pi})/\Delta t$, which is determined by slopes of the tangents to the onset curves of Fig. 3. The P1 region exhibits a faster onset rate, and its decay follows an exponential behavior beginning with the trailing edge of the e-beam pulse (time$\approx$0). The P2 region, conversely, exhibits a slow onset and its CL intensity decays very slowly during the first $\sim$1 ns after the trailing edge of the e-beam pulse and then proceeds to decay exponentially. This unusual delayed decay behavior was observed consistently for other dark valley regions which were found in close proximity ($\sim$1 μm) of sharp peaks. This delayed time ranged from 0.2–1.0 ns.

The different onset rates of P1 and P2 as well as the delay for P2 can be explained by considering a simple model that involves carrier generation in dark boundary regions and transport to the lower band gap InN-rich centers that yield the high exciton localization. At the trailing edge of the e-beam excitation, excess carriers can diffuse and drift from the higher to lower band gap regions. Thus, we expect the field-induced drift of carriers to play an important role in funneling and collection of carriers at the InN-rich centers. At the trailing edge of the e-beam pulse, generated carriers in the higher band gap dark regions (P2) must traverse the 0.1–1.0 μm distance prior to collection and recombination in the InN-rich centers. This process gives rise to the apparent 0.2–1.0 ns delay in the CL transient as carriers are continuously fed to the luminescence centers. This process likewise explains the slower onset rate of P2, as the onset is delayed by the initial carrier transport to the InN-rich centers. The relative proximity of the e-beam position to the centers will influence the measured delay. After diffusion and drift to the InN-rich centers, the carriers can recombine radiatively. Owing to possible nonradiative centers in the boundary regions, carrier loss during transport is expected to occur and contributes to the reduced lifetime measured in dark regions. The rapid band filling observed in Fig. 1 and the excitation dependence of the feature size are also consistent with the notion of spatially segregated InN-rich centers with a high carrier collection efficiency. The collection of carriers at dispersed centers will naturally lead to an enhanced phase space filling due to the enhanced real space filling (i.e., funneling of carriers) in the centers. These results indicate a high capture and luminescence efficiency in InN-rich centers and further help to explain the high efficiency of optoelectronic devices based on InGaN alloys, despite high densities of structural defects.[13]

In conclusion, we have examined the optical properties and kinetics of carrier relaxation for an InGaN QW sample with spatially, spectrally, and temporally resolved CL. CLWI reveals a spatial variation in the near-band gap energy resulting from the In composition undulation throughout the InGaN film. The lifetime of carriers excited in dark regions located between the InN-rich centers is reduced and a 0.2–1.0 ns delay in the transient decay signal is observed, owing to diffusion and drift of carriers. The lateral band gap variation throughout the QW can lead to interesting nonlinear optical effects which could impact applications involving lasers, optical storage, and spatial light modulators.

This work was supported by NSF, ARO, ONR, and DARPA through the National Center for Integrated Photonic Technology (NCIPT).

[1] S. Nakamura, M. Senoh, N. Iwasa, S. Nagahama, T. Yamada, and T. Mukai, Jpn. J. Appl. Phys., Part 2 **134**, L1332 (1994).
[2] S. Nakamura, M. Senoh, S. Nagahama, N. Iwasa, T. Yamada, T. Matsushita, H. Kiyoku, and Y. Sugimoto, Appl. Phys. Lett. **68**, 3269 (1996).
[3] L. Akasaki, S. Sota, H. Sakai, T. Tanaka, M. Koike, and H. Amano, Electron. Lett. **32**, 1105 (1996).
[4] C.-K. Sun, S. Keller, G. Wang, M. S. Minsky, J. E. Bowers, and S. P. DenBarrs, Appl. Phys. Lett. **69**, 1936 (1996).
[5] E. S. Jeon, V. Kozalov, Y.-K. Song, A. Vertikov, M. Kuball, A. V. Nurmikko, H. Liu, C. Chen, R. S. Kern, C. P. Kuo, and M. G. Craford, Appl. Phys. Lett. **69**, 4194 (1996).
[6] Y. Narukawa, Y. Kawakami, S. Fujita, and S. Fujita, Phys. Rev. B **55**, R1938 (1997).
[7] Y. Narukawa, Y. Kawakami, M. Funato, S. Fujita, and S. Fujita, Appl. Phys. Lett. **70**, 981 (1997).
[8] S. Chichibu, T. Azuhata, T. Sota, and S. Nakamura, Appl. Phys. Lett. **69**, 4188 (1996).
[9] S. Chichibu, K. Wada, and S. Nakamura, Appl. Phys. Lett. **71**, 2346 (1997).
[10] K. Rammohan, D. H. Rich, R. S. Goldman, J. Chen, H. H. Wieder, and K. L. Kavanagh, Appl. Phys. Lett. **66**, 869 (1995).
[11] J. T. Kobayashi, N. P. Kobayashi, P. D. Dapkus, X. Zhang, and D. H. Rich, Mater. Res. Soc. Symp. Proc. **468**, 187 (1997).
[12] H. T. Lin, D. H. Rich, A. Konkar, P. Chen, and A. Madhukar, J. Appl. Phys. **81**, 3186 (1997).
[13] S. D. Lester, F. A. Ponce, M. G. Craford, and D. A. Steigerwald, Appl. Phys. Lett. **66**, 1249 (1995).